Inorg. Chem. **2007**, *46*, 4917–4925

Infrared Spectrum and Bonding in Uranium Methylidene Dihydride, $CH_2{=}UH_2$

Jonathan T. Lyon and Lester Andrews*

Department of Chemistry, P.O. Box 400319, Charlottesville, Virginia 22904-4319

Per-Åke Malmqvist and Björn O. Roos

Department of Theoretical Chemistry, Chemical Center, POB 124, S-221 00, Lund, Sweden

Tianxiao Yang and Bruce E. Bursten

Department of Chemistry, The Ohio State University, Columbus, Ohio 43210

Received December 15, 2006

Uranium atoms activate methane upon ultraviolet excitation to form the methyl uranium hydride CH_3–UH, which undergoes α-H transfer to produce uranium methylidene dihydride, $CH_2{=}UH_2$. This rearrangement most likely occurs on an excited-quintet potential-energy surface and is followed by relaxation in the argon matrix. These simple U + CH_4 reaction products are identified through isotopic substitution ($^{13}CH_4$, CD_4, CH_2D_2) and density functional theory frequency and structure calculations for the strong U–H stretching modes. Relativistic multiconfiguration (CASSCF/CASPT2) calculations substantiate the agostic distorted C_1 ground-state structure for the triplet $CH_2{=}UH_2$ molecule. We find that uranium atoms are less reactive in methane activation than thorium atoms. Our calculations show that the $CH_2{=}UH_2$ complex is distorted more than $CH_2{=}ThH_2$. A favorable interaction between the low energy open-shell U(5f) σ orbital and the agostic hydrogen contributes to the distortion in the uranium methylidene complexes.

Introduction

Uranium chemistry is important because of our need for energy from nuclear sources, the associated engineering problems with containment and environmental concerns, and for the detection of nuclear explosives.[1−3] Uranium is the third actinide metal, and its chemistry may be related to that of the group 6 transition metals.[4]

Transition-metal complexes with carbon−metal double bonds are important in metal coordination chemistry and for use as catalysts in alkene metathesis and alkane activation reactions.[5−7] Many early transition-metal alkylidenes exhibit the agostic interaction of hydrogen with a transition-metal center.[7−11] The simplest example of this interaction is the methylidene dihydride, $CH_2{=}MH_2$, which provides an ideal model system to examine substituent effects and the agostic interaction with a variety of transition metals. Groups 4 and 5, and particularly group 6 alkylidene complexes have been characterized,[7] but the corresponding actinide alkylidene complexes have not been prepared,[12] although uranium−carbon multiple-bonded complexes and surface-stabilized actinide alkylidene species have been reported.[13,14] Increased

* To whom correspondence should be addressed. E-mail: lsa@virginia.edu.

(1) Wilson, E. K. *Chem. Eng. News.*, **2005**, *83* (Oct 10), 40.
(2) Myers, W.; Elkins, N. *Nuclear News*, Dec 33, 2004, and references therein.
(3) Erten, H. N.; Mohammed, A. K.; Choppin, G. R. *Radiochim. Acta* **1994**, *66/67*, 123.
(4) Cotton, F. A.; Wilkinson, G.; Murillo, C. A.; Bochmann, M. *Advanced Inorganic Chemistry*, 6th ed.; Wiley & Sons: New York, 1999.
(5) Grubbs, R. H.; Coates, G. W. *Acc. Chem. Res.* **1996**, *29*, 85.
(6) Buchmeiser, M. R. *Chem. Rev.* **2000**, *100*, 1565.
(7) Schrock, R. R. *Chem. Rev.* **2002**, *102*, 145.
(8) Crabtree, R. H. *Chem. Rev.* **1985**, *85*, 245.
(9) Ujaque, G.; Cooper, A. C.; Maseras, F.; Eisenstein, O.; Caulton, K. G. *J. Am. Chem. Soc.* **1998**, *120*, 361.
(10) Wada, K.; Craig, B.; Pamplin, C. B.; Legzdins, P.; Patrick, B. O.; Tsyba, I.; Bau, R. *J. Am. Chem. Soc.* **2003**, *125*, 7035.
(11) Scherer, W.; McGrady, G. S. *Angew. Chem., Int. Ed.* **2004**, *43*, 1782.
(12) (a) Pool, J. A.; Scott, B. L.; Kiplinger, J. L. *J. Am. Chem. Soc.* **2005**, *127*, 1338. (b) Burns, C. J. *Science* **2005**, *309*, 1823.
(13) See, for example, Cramer, R. E.; Maynard, R. B.; Paw, J. C.; Gilje, J. W. *J. Am. Chem. Soc.* **1981**, *103*, 3589.

10.1021/ic062407w CCC: $37.00
Published on Web 05/08/2007

reactivity of actinide alkylidenes may make them difficult to prepare using conventional synthetic methods, but the solid argon matrix environment can isolate and prepare these compounds.

Laser-ablated Zr atoms activated CH_4 to form the CH_3-ZrH insertion product, which rearranged by α-H transfer to the methylidene dihydride $CH_2=ZrH_2$ complex.[15] This methylidene was determined from its matrix infrared spectrum using isotopic substitution and electronic structure calculations to exhibit CH_2 and ZrH_2 distortion, which is characteristic of the agostic interaction.[9,11] This distortion was measured through the H′−C−Zr angle computed as 92.9° at the B3LYP level and 83.8° at the CCSD(T) level.[15,16] A similar investigation with the actinide Th found methane activation to form the analogous thorium methylidene $CH_2=ThH_2$ with a 95.6° agostic H′−C−Th angle at the B3LYP level and 93.1° at the CCSD level.[17] A recent theoretical investigation predicted that the insertion of Th into the C−H bond of methane would be essentially barrierless and considerably exothermic.[18] Moving to the right two rows in the periodic table, laser-ablated Mo atoms activate methane to form CH_3-MoH, $CH_2=MoH_2$, and $CH\equiv MoH_3$, which rearrange through photoreversible α-H transfer, and W atoms form the analogous complexes. The tungsten methylidene exhibits weaker agostic bonding effects with a 91.0° agostic H′−C−W angle computed at the CCSD level. Both group 6 metals exhibit weaker agostic interactions, on the basis of the computed H′−C−M angles in the $CH_2=MH_2$ methylidene dihydrides, than their group 4 counterparts.[19]

It is therefore of considerable interest to compare the reactivity of U and Th in methane activation. To this end, we prepare the simple uranium methylidene dihydride or uranoethylene, $CH_2=UH_2$, confirm its stability, calculate its structure for possible agostic distortion, and determine that further α-H transfer to the hexavalent $CH\equiv UH_3$ methylidyne species does not happen in this system. Multiconfiguration character and spin−orbit coupling may be important for the anticipated triplet-state $CH_2=UH_2$ molecule, so we also compare the results of DFT calculations and the more rigorous CASSCF/CASPT2 method, as has been reported for the triplet-state UO_2 molecule.[20]

Methods

The matrix-isolation apparatus has been described previously.[15,21,22] Laser-ablated (Nd:YAG laser operating at 1064 nm, 10 Hz repetition rate, 10 ns pulse width) uranium atoms were reacted with methane and isotopic samples ($^{13}CH_4$, CD_4, CH_2D_2) diluted in argon during co-deposition onto an 8 K substrate. Infrared spectra were recorded on a Nicolet 550 FTIR after sample deposition, after annealing, and after irradiation using a mercury arc lamp.

The structures and vibrational frequencies of product molecules, the anticipated quintet insertion product CH_3-UH, and the triplet methylidene $CH_2=UH_2$ complex were calculated using density functional theory (DFT). We performed the DFT calculations with the B3LYP density functional,[23] the 6-311++G(2d,p) basis sets,[24,25] SDD pseudopotential (32 valence electrons)[26] in the Gaussian 98 system[27] as well as the PW91 functional,[28,29] and the uncontracted STO basis sets of triple-ζ quality[30] with the ADF code.[31] All of the ADF geometries were fully optimized with the inclusion of scalar relativistic effects. Vibrational frequencies and infrared intensities were determined via numerical evaluation of the second-order derivatives of the total energies. A numerical integration accuracy of integration = 10.0 was used throughout, together with very tight convergence criteria for energy iterations and for geometry optimizations.

To investigate the spin−orbit coupling effects in the $CH_2=UH_2$ complex, we performed ab initio spin−orbit configuration interaction (SOCI) calculations with the Columbus suite of programs.[32,33] The electron correlation and spin−orbit interaction are treated simultaneously by the multireference CI method. The RECPs of uranium and carbon atoms used in this work are those developed by Christiansen and co-workers.[34−36] The uranium core is 1s through 5p shells (68 electrons). The carbon core is 1s shell (2 electrons). Thus, in $CH_2=UH_2$, 32 valence electrons are treated explicitly. The correlation-consistent polarized-valence double-ζ (cc-pVDZ) basis

(14) He, M.-Y.; Xiong, G.; Toscano, P. J.; Burwell, R. L., Jr.; Marks, T. J. *J. Am. Chem. Soc.* **1985**, *107*, 641.
(15) Cho, H.-G.; Wang, X.; Andrews, L. *J. Am. Chem. Soc.* **2005**, *127*, 465 (CH_4 + Zr).
(16) Andrews, L.; Cho, H.-G. *Organometallics* **2006**, *25*, 4040 (review article).
(17) Andrews, L.; Cho, H.-G. *J. Phys. Chem. A* **2005**, *109*, 6796 (CH_4 + Th).
(18) de Almeida, K. J.; Cesar, A. *Organometallics* **2006**, *25*, 3407.
(19) (a) Cho, H-G.; Andrews, L. *J. Am. Chem. Soc.* **2005**, *127*, 8226 (CH_4 + Mo). (b) Cho, H.-G.; Andrews, L.; Marsden, C. *Inorg. Chem.* **2005**, *44*, 7634 (CH_4 + W). (c) Roos, B. O.; Lindh, R. H.; Cho, H.-G.; Andrews, L. *J. Phys. Chem. A*, **2007**, in press.
(20) Gagliardi, L.; Roos, B. O.; Malmqvist, P.-Å.; Dyke, J. M. *J. Phys. Chem. A* **2001**, *105*, 10602.
(21) Andrews, L. *Chem. Soc. Rev.* **2004**, *33*, 123.
(22) Hunt, R. D.; Andrews, L. *J. Chem. Phys.* **1993**, *98*, 3690.
(23) (a) Becke, A. D. *J. Chem. Phys*. **1993**, *98*, 5648. (b) Lee, C.; Yang, E.; Parr, R. G. *Phys. Rev. B* **1988**, *37*, 785.
(24) Stevens, P. J.; Devlin, F. J.; Chablowski, C. F.; Frisch, M. J. *J. Phys. Chem*. **1994**, *98*, 11623.
(25) Frisch, M. J.; Pople, J. A.; Binkley, J. S. *J. Chem. Phys.* **1984**, *80*, 3265.
(26) Küchle, W.; Dolg, M.; Stoll, H.; Preuss, H. *J. Chem. Phys.* **1994**, *100*, 7535.
(27) Frisch, M. J.; Trucks, G. W.; Schlegel, H. B.; Scuseria, G. E.; Robb, M. A.; Cheeseman, J. R.; Zakrzewski, V. G.; Montgomery, J. A., Jr.; Stratmann, R. E.; Burant, J. C.; Dapprich, S.; Millam, J. M.; Daniels, A. D.; Kudin, K. N.; Strain, M. C.; Farkas, O.; Tomasi, J.; Barone, V.; Cossi, M.; Cammi, R.; Mennucci, B.; Pomelli, C.; Adamo, C.; Clifford, S.; Ochterski, J.; Petersson, G. A.; Ayala, P. Y.; Cui, Q.; Morokuma, K.; Malick, D. K.; Rabuck, A. D.; Raghavachari, K.; Foresman, J. B.; Cioslowski, J.; Ortiz, J. V.; Stefanov, B. B.; Liu, G.; Liashenko, A.; Piskorz, P.; Komaromi, I.; Gomperts, R.; Martin, R. L.; Fox, D. J.; Keith, T.; Al-Laham, M. A.; Peng, C. Y.; Nanayakkara, A.; Gonzalez, C.; Challacombe, M.; Gill, P. M. W.; Johnson, B. G.; Chen, W.; Wong, M. W.; Andres, J. L.; Head-Gordon, M.; Replogle, E. S.; Pople, J. A. *Gaussian 98*, revision A.11.4; Gaussian, Inc.: Pittsburgh, PA, 2002.
(28) Perdew, J. P.; Wang, Y. *Phys. Rev. B* **1992**, *45*, 13244.
(29) Perdew, J. P.; Chevary, J. A.; Vosko, S. H.; Jackson, K. A.; Peterson, M. R.; Singh, D. J.; Foilhais, C. *Phys. Rev. B* **1992**, *46*, 6671.
(30) van Lenthe, E.; Baerends, E. J. *J. Comput. Chem*. **2003**, *24*, 1142.
(31) ADF 2004.01, Theoretical Chemistry, Vrije Universiteit, Amsterdam, referenced in (a) Baerends, E. J.; Ellis, D. E.; Ros, P. *Chem. Phys.* **1973**, *2*, 42. (b) te Velde, G.; Baerends, E. J. *J. Comput. Phys.* **1992**, *99*, 94. (c) Fonseca Guerra, C.; Visser, O.; Snijders, J. G.; te Velde, G.; Baerends, E. J. In *Methods and Techniques for Computational Chemistry;* Clementi, E., Corongiu, G., Eds.; STEF: Cagliari, Italy, 1995; p 305.
(32) See http://www.univie.ac.at/columbus/ for information on the Columbus programs.
(33) Yabushita, S.; Zhang, Z.; Pitzer, R. M. *J. Phys. Chem. A* **1999**, *103*, 5791.
(34) See http://people.clarkson.edu/~pac/reps.html for complete references and a library of potentials.
(35) Ermler, W. C.; Ross, R. B.; Christiansen, P. A. *Int. J. Quantum Chem.* **1991**, *40*, 829.
(36) Pacios, L. F.; Christiansen, P. A. *J. Chem. Phys*. **1985**, *82*, 2664.

sets were used for U,[37] C,[38−40], and H[41] atoms. Because SOCI calculations are computationally intensive, full geometry optimizations for the $CH_2{=}UH_2$ molecule are not feasible at this level of theory, so we used the ADF optimized geometries. In the ADF calculations, a total of 22 electrons were correlated, which include 14 U electrons in the 6s, 6p, 5f, 6d, and 7s orbitals, 4 C electrons in the 2s and 2p orbitals, and 4 H electrons in the 1s orbitals. Next, we optimized the geometries using CASSCF/CASPT2 methods[42,43] and calculated energies with spin−orbit correction as described in a recent report.[44] A relativistic ANO-RCC basis set was used of the size 9s8p6d4f2g for Th and U, 4s3p2d1f for C, and 3s2p for hydrogen.[45] The active space included the actinide-carbon and actinide-hydrogen bonding and antibonding orbitals (eight orbitals with eight electrons) plus the two open-shell electrons for the uranium system. The CH bonds were left inactive. The geometry was optimized at the CASPT2 level of theory using numerical gradients. Spin−orbit calculations were performed at the optimized geometries using the RASSI-SO method.[46]

Results and Discussion

Matrix infrared investigation of the U atom and methane reaction products will be presented along with quantum chemical calculations of anticipated product molecules at several levels of quantum chemical theory.

Infrared Spectra. The reaction of laser-ablated uranium atoms and methane was investigated in five argon matrix-isolation experiments using a range of sample concentrations and laser energies, and infrared spectra from the 2.5% CH_4 sample are illustrated in Figure 1. Weak new 1425.4 and 1368.0 cm^{-1} bands are observed on sample deposition along with a trace of HO_2 radical, NUN, Ar_nH^+, UO_2, CH_3 radical, C_2H_2, C_2H_4, and C_2H_6.[22,47−53] The 1425.4 cm^{-1} band increases with $\lambda > 290$ nm irradiation and acquires a partner at 1461.2 cm^{-1}, but the 1368.0 cm^{-1} feature changes little; however, with $\lambda > 220$ nm irradiation the 1461.2 and 1425.4 cm^{-1} pair (labeled **m**) increases 3-fold, and the 1368.0 cm^{-1} feature (labeled **i**) increases slightly. A broader satellite absorption appears at 1416.5 cm^{-1}. Subsequent annealing at 30 K sharpens the **m** bands, and they decrease together on annealing at 35 K. No significant other absorptions are observed in the spectra.

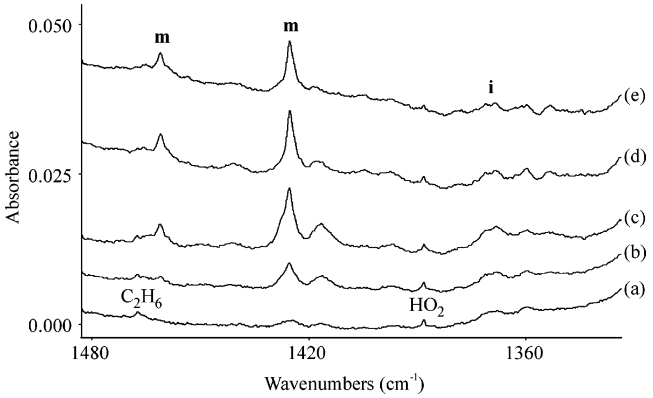

Figure 1. Infrared spectra in the 1480−1340 cm^{-1} region for laser-ablated uranium and methane reaction products in excess argon at 8 K. (a) U + 2.5% CH_4 in argon deposited for 60 min, (b) after $\lambda > 290$ nm irradiation for 20 min, (c) after $\lambda > 220$ nm irradiation for 20 min, (d) after annealing to 30 K, and (e) after annealing to 35 K.

A similar reaction with $^{13}CH_4$ gave the same new product absorptions to 0.1 cm^{-1}. Three investigations with CD_4 gave a weak new 1044.2 cm^{-1} band and a 1016 cm^{-1} shoulder absorption above the strong 994 cm^{-1} CD_4 precursor absorption and at 977.4 cm^{-1} below. These bands exhibited the same photochemical and annealing behavior as their CH_4 **m** and **i** counterparts. Two experiments with 5% CH_2D_2 produced weak absorptions at 1461.2 and 1453.6 cm^{-1} above and at 1368.0 cm^{-1} below the strong 1431 cm^{-1} reagent absorption and at 1044.0 cm^{-1} above and at 977.4 cm^{-1} below the 1032 cm^{-1} reagent band. Again, the same photochemical and annealing behavior was found.

The new **m** and **i** bands fall in the region expected for U−H stretching frequencies,[54] and this mode description is substantiated by the H/D isotopic frequency ratios (1.3993, 1.40, and 1.3996) and the absence of any carbon-13 shift. The sharp **m** bands track together with changes in CH_4 concentration up to 10% and laser energy giving U concentration at least 2-fold higher; accordingly, the two **m** bands are due to two U−H stretching fundamentals of a single new molecule. Only the higher-frequency **m** bands analogous to bands from CH_4 and CD_4 experiments could be observed with CH_2D_2 because of masking by precursor absorptions, but the same **i** absorptions were observed unshifted from CH_4 and CD_4 investigations. Thus, the broader **i** absorptions appear to be due to the single U−H stretching mode of another molecule with different photochemistry. The new 1453.6 cm^{-1} band with CH_2D_2 is due to the U−H stretching mode in a UHD subunit, and unfortunately the CH_2D_2 absorption masks the U−D counterpart. Observation of the same **i** bands with CH_4, CH_2D_2, and CD_4 provides evidence for a single U−H(D) stretching mode.

Theoretical Calculations and Product Assignments. Following the example of methane activation products with Zr, Mo, and Th,[15−17,19] we performed density functional

(37) Brozell, S. R. Ph.D. Dissertation, The Ohio State University, 1999, p 67.
(38) See http://www.chemistry.ohio-state.edu/~pitzer/basis_sets.html for complete information.
(39) Wallare, N. W.; Blaudeau, J-P.; Pitzer, R. M. *Int. J. Quantum Chem.* **1991**, *40*, 789.
(40) Christiansen, P. A. *J. Chem. Phys.* **2000**, *112*, 10070.
(41) Dunning, T. H. *J. Chem. Phys.* **1989**, *90*, 1007.
(42) Roos, B. O. Ab Innitio Methods in Quantum Chemistry − II. In *Advances in Chemical Physics;* Lawly, K. P., Ed.; Wiley & Sons: Chichester, U.K., 1987; pp 399−445.
(43) Andersson, K.; Malmqvist, P.-Å.; Roos, B. O.; Sadlej, A. J.; Wolinski, K. J. *J. Phys. Chem.* **1990**, *94*, 5483.
(44) Gagliardi, L.; Roos, B. O. *Nature* **2005**, *433*, 848.
(45) Roos, B. O.; Lindh, R.; Malmqvist, P.-Å.;Veryazov, V.; Widmark, P.-O. *Chem. Phys. Letters* **2005**, *409*, 295.
(46) Roos, B. O.; Malmqvist, P.-Å. *Phys. Chem. Chem. Phys.* **2004**, *6*, 2919.
(47) (a) Milligan, D. E.; Jacox, M. E. *J. Chem. Phys.* **1963**, *38*, 2627. (b) Smith, D. W.; Andrews, L. *J. Chem. Phys.* **1974**, *60*, 81.
(48) (a) Hunt, R. D.; Yustein, J. T.; Andrews, L. *J. Chem. Phys.* **1993**, 6070. (b) Zhou, M.; Andrews, L.; Li, J.; Bursten, B. E. *J. Am. Chem. Soc.* **1999**, *121*, 12188.
(49) Wight, C. A.; Ault, B. S.; Andrews, L. *J. Chem. Phys.* **1976**, *65*, 1244.
(50) Jacox, M. E. *J. Mol. Spectrosc.* **1977**, *66*, 272.
(51) Wang, X.; Andrews, L. *J. Phys. Chem. A* **2003**, *107*, 337.
(52) Cho, H.-G.; Andrews, L. *J. Phys. Chem. A* **2004**, *108*, 3965.
(53) Davis, S. R.; Andrews, L. *J. Am. Chem. Soc.* **1987**, *109*, 4768.
(54) Souter, P. F.; Kushto, G. P.; Andrews, L.; Neurock, M. *J. Am. Chem. Soc.* **1997**, *119*, 1682.

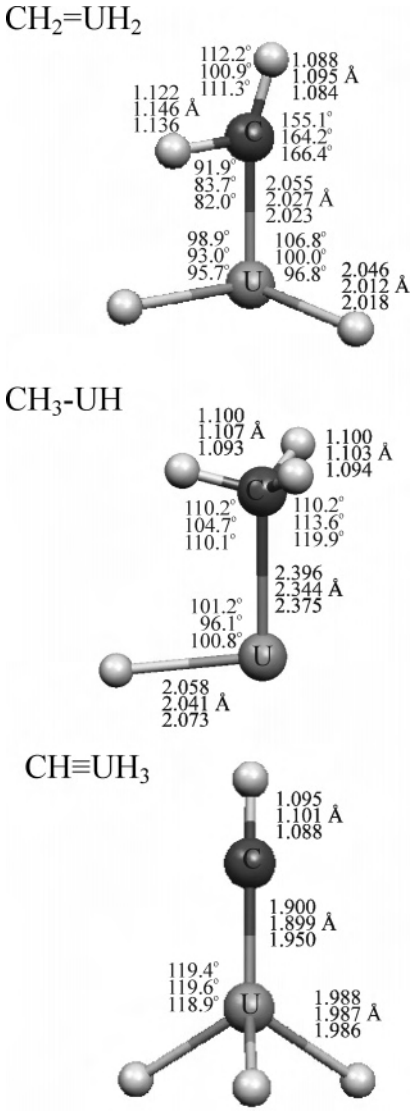

Figure 2. Structures calculated for CH_3-UH, $CH_2=UH_2$, and $CH\equiv UH_3$ using (a) the B3LYP (Gaussian) and (b) the PW9l (ADF) density functionals and (c) the CASSCF/CASPT2 methods. Parameters (bond lengths in angstroms and angles in degrees) calculated by these three methods are given from top to middle to bottom, respectively.

calculations using the B3LYP and BPW91 functionals for the quintet insertion product CH_3-UH and the triplet methylidene $CH_2=UH_2$ formed by subsequent α-H transfer. Similar ADF calculations for uranium oxyhydrides and oxyhydroxides gave good frequency agreement with experiment.[55,56]

The quintet methyl uranium hydride is the global minimum-energy primary product with a plane of symmetry, a long C−U single bond length of 2.396 Å, a U−H bond length of 2.058 Å, and one very strong infrared absorption for the U−H stretching mode computed at 1370 cm^{-1} (558 km/mol) at the B3LYP level or at 1416 cm^{-1} (374 km/mol) with the PW91/ADF system. The calculated structures and parameters are illustrated in Figure 2. Other frequencies of CH_3-UH are computed to be too weak or too low in frequency to be observed here. The weak 1368.0 cm^{-1} absorption labeled **i** increases slightly on UV irradiation and can reasonably be assigned to the strongest absorption of CH_3-UH, which is the anticipated first-reaction product. The 977.4 cm^{-1} CD_4 counterpart defines the H/D isotopic frequency ratio 1.3997, which is appropriate for a heavy-metal−hydrogen stretching mode. The observation of both 1368.0 and 977.4 cm^{-1} bands with CH_2D_2 is in agreement with this assignment. Our calculations show that the replacement of H with D in the methyl group does not alter the U−H stretching mode. Note that the CH_3-UH structures are computed to be very similar by the B3LYP, PW91, and CASPT2 methods (Figure 2).

The distorted triplet methylidene dihydride $CH_2=UH_2$ (Figure 2) has a C=U double bond length of 2.055 Å, an agostic H′−C−U angle of 91.9°, U−H bonds lengths of 2.024 and 2.040 Å, and two strong U−H stretching frequencies computed at 1479.3 cm^{-1} (460 km/mol) and 1437.1 cm^{-1} (665 km/mol), all using the B3LYP functional (Table 1). The next-strongest absorption, the U=C stretching mode, is computed at 653.9 cm^{-1} with only 20% of the intensity of the strongest absorption. The PW91 calculation predicts slightly higher strong U−H stretching absorptions at 1504.5 and 1462.0 cm^{-1} and a similar structure with more agostic distortion (Figure 2). Furthermore, the ADF calculations find the C_1 symmetry structure 1 kcal/mol lower than the corresponding C_s structure with a symmetry plane bisecting the CH_2 and UH_2 angles. Analogous quintet CH_2-UH_2 structures in C_1 and C_s symmetries are 28 and 25 kcal/mol higher in energy than the triplet $CH_2=UH_2$ structure, respectively. Next, we optimized the geometry for $CH_2=UH_2$ at the MP2//6-311++G(2d,p)/SDD level[57] using Gaussian 98 and found that the MP2-optimized structure has even more agostic distortion and is closer to the ADF-optimized structure than the B3LYP-optimized structure (H′−C−U angle 81.7°, C−H: 1.140, 1.088 Å, C−U: 2.018 Å, U−H: 1.985, 1.989 Å). A recent comparative investigation of agostic bonding in $CH_2=TiHF$ found the MP2 method overestimates the agostic distortion effect.[58]

Next, we performed CASSCF/CASPT2 calculations for $CH_2=UH_2$ and CH_3-UH, and the structural parameters are compared in Figure 2. This more rigorously determined methylidene structure is considerably distorted with parameters between the PW91 and MP2 values. The methylidene is 15 kcal/mol higher in energy than the inserted hydride at this level of theory without the inclusion of spin−orbit coupling, but with spin−orbit coupling this energy difference is only 1 kcal/mol. Finally, the $CH_2=UH_2$ structure contributes 96% to the ground-state triplet configuration, and the molecular orbitals calculated with the CASPT2 method are shown in Figure 3.

(55) Liang, B.; Hunt, R. D.; Kushto, G. P.; Andrews, L.; Li, J.; Bursten, B. E. *Inorg. Chem.* **2005**, *44*, 2159.
(56) Wang, X.; Andrews, L.; Li, J. *Inorg. Chem.* **2006**, *45*, 4157.
(57) (a) Head-Gordon, M.; Pople, J. A.; Frisch, M. J. *Chem. Phys. Lett.* **1988**, *153*, 503. (b) Frisch, M. J.; Head-Gordon, M.; Pople, J. A. *Chem. Phys. Lett.* **1990**, *166*, 275. (c) Frisch, M. J.; Head-Gordon, M.; Pople, J. A. *Chem. Phys. Lett.* **1990**, *166*, 281. (d) Head-Gordon, M.; Head-Gordon, T. *Chem. Phys. Lett.* **1994**, *220*, 122. (e) Saebo, S.; Almlof, J. *Chem. Phys. Lett.* **1989**, *154*, 83.
(58) von Frantzius, G.; Streubel, R.; Brandhorst, K.; Grunenberg, J. *Organometallics* **2006**, *25*, 118.

Table 1. Observed and Calculated Fundamental Frequencies of $CH_2{=}UH_2$

approximate mode	$CH_2{=}UH_2$							$^{13}CH_2{=}UH_2$			$CD_2{=}UD_2$		
description	obsd	calcd[a]	int.[a]	calcd[b]	int.[b]	calcd[c]	int.[c]	obsd	calcd[a]	int.[a]	obsd	calc[a]	int.[a]
CH_2 stretch		3137.8	1	3071.7	1	3062.7	4		3127.4	1		2318.2	2
CH_2 stretch		2804	6	2631.7	3	2591.2	3		2797.4	7		2041.5	1
UH_2 stretch	1461.1	1479.3	460	1468.2	393	1504.5	413	1461.1	1479.3	460	1044.2	1049	229
UH_2 stretch	1425.4	1437.1	665	1417.0	561	1462.0	478	1425.4	1437.1	664	1016 sh	1019.4	345
CH_2 bend		1340.6	22	1335.5	21	1352.7	19		1333	21		1022.6	22
U=C stretch		653.9	138	658.4	127	701.3	135		636.5	136		585	88
CH_2 wag		607.1	127	593.7	69	591.9	112		601.3	123		476.8	89
UH_2 bend		517	82	575.7	69	639.4	16		514.7	85		389.4	24
UH_2 rock		477.5	60	438.0	59	488.8	40		475.7	56		345.6	49
CH_2 twist		392.8	33	413.8	66	442.2	34		392.5	32		279.8	20
UH_2 wag		320.9	80	259.1	41	296.0	22		320.6	79		228.6	39
CH_2 rock		217.3	40	150.9	78	235.5	42		217.1	40		154.4	20

[a] Gaussian 98/B3LYP//6-311++G(2d,p)/SDD level of theory. [b] Gaussian 98/BPW91//6-311++G(2d,p)/SDD level of theory. [c] ADF//PW91 level of theory (intensity). All of the frequencies and infrared intensities are in cm^{-1} and km/mol. Observed values are in an argon matrix.

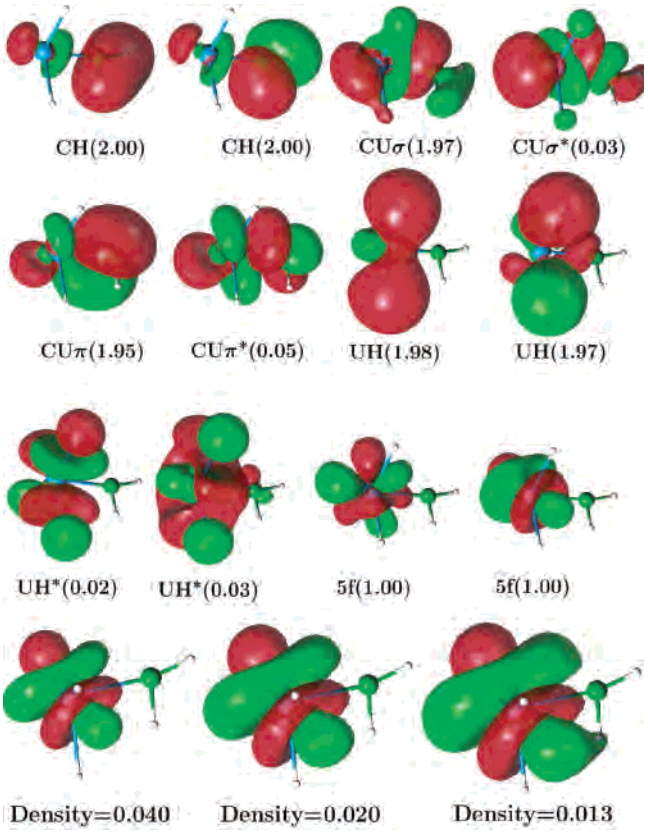

Figure 3. (A) Twelve molecular orbitals for $CH_2{=}UH_2$ computed at the CASSCF/CASPT2 level of theory. The numbers in parentheses are electron occupations. (B) Three more-sensitive electron-density plots for the U(5f) σ orbital showing agostic interaction.

Considering that DFT is a single-reference method without spin−orbit coupling, we also computed the electronic structure of $CH_2{=}UH_2$ using the ab initio SOCI method. We performed multireference CISD calculations. The MRCISD results are energy consistent with those of the DFT method. The agostic distorted C_1 symmetry structure is 3 kcal/mol lower than the C_s symmetry structure. This illustrates that after inclusion of the spin−orbit coupling, the electronic-energy order for these $CH_2{=}UH_2$ structures does not change. The agostic distorted C_1 structure is the global minimum energy for the triplet $CH_2{=}UH_2$ molecule, and the distorted structure converged using the CASPT2 method is given in Figure 2. Experience has shown that the inclusion of spin−orbit coupling has little effect on the calculated geometry.[20]

Electronic structure calculations at different levels of theory can provide vibrational frequencies, which approximate experimental values with different degrees of accuracy. Density functional theory is particularly effective for the prediction of vibrational frequencies for new molecules including those containing actinide metal atoms.[55,59,60] Table 1 compares sets of frequencies computed by the Gaussian//B3LYP, Gaussian//BPW91, and ADF//PW91 density functional methods for $CH_2{=}UH_2$ with the observed U−H stretching frequencies. The B3LYP frequencies are 1.2 and 0.8% higher, the BPW91 values are +0.5 and −0.6%, and the PW91 frequencies are 2.9 and 2.5% higher than experimental values. This is the range of agreement for DFT frequency predictions not corrected for anharmonicity.[61] Similar agreement between calculated and observed frequencies is found for $CH_2{=}ThH_2$ (Table 2) where Gaussian//B3LYP frequencies are 0.1 and 0.2% lower, Gaussian//BPW91 frequencies are 0.9 and 0.7% lower, and ADF//PW91 frequencies are 1.0 and 1.0% higher than experimental values. These three methods also predict the C=Th stretching and CH_2 wagging modes: 1.3% high, 0.3% low, 3.0% high, 6.6% low, and 3.0% high, 3.8% low, respectively. In the case of $CH_2{=}ThH_2$, we were able to compute vibrational frequencies using the more rigorous CCSD[16,17,62] method in Gaussian 98, and the CCSD frequencies are slightly higher than the values computed by DFT (Table 2). For example, the CCSD-calculated Th−H stretching frequencies are 2.7 and 3.5% higher than the observed values. This comparison substantiates the use of the less-time-consuming DFT methods for computation of vibrational frequencies for actinide-metal-containing molecules.

(59) Zhou, M.; Andrews, L.; Li, J.; Bursten, B. E. *J. Am. Chem. Soc.* **1999**, *121*, 9712.
(60) Zhou, M.; Andrews, L.; Ismail, N.; Marsden, C. *J. Phys. Chem. A* **2000**, *104*, 5495.
(61) Scott, A. P.; Radom, L. *J. Phys. Chem.* **1996**, *100*, 16502.
(62) (a) Cizek, J. *Adv. Chem. Phys*. **1969**, *14*, 35. (b) Purvis, G. D.; Bartlett, R. J. *J. Chem. Phys.* **1982**, *76*, 1910. (c) Scuseria, G. E.; Janssen, C. L.; Schaefer, H. F., III. *J. Chem. Phys.* **1988**, *89*, 7382. (d) Scuseria, G. E.; Schaefer, H. F., III. *J. Chem. Phys.* **1989**, *90*, 3700.

Table 2. Observed and Calculated Fundamental Frequencies of $CH_2{=}ThH_2$[a]

approximate mode	obsd	calcd[b]	int.[b]	calcd[c]	int.[c]	calcd[d]	int.[d]	calcd[e]	int.[e]
CH_2 stretch		3164.7	3	3078.7	0.3	3142.6	2	3080.0	2
CH_2 stretch		2853.4	14	2726.1	5	2861.4	11	2747.7	6
ThH_2 stretch	1435.7	1476.0	400	1450.9	295	1434.9	350	1422.1	305
ThH_2 stretch	1397.1	1448.1	709	1413.0	607	1394.2	698	1387.3	619
CH_2 bend		1371.0	8	1306.0	35	1327.5	11	1301.3	20
C=Th stretch	670.8	685.5	80	691.2	160	679.6	178	690.8	165
CH_2 wag	634.6	636.2	203	611.4	139	633.0	161	592.5	147
ThH_2 bend	458.7	540.3	70	508.5	24	492.8	110	495.0	38
ThH_2 rock		481.7	17	479.3	67	460.8	5	472.9	59
CH_2 twist		383.5	26	396.1	29	343.0	30	387.8	30
ThH_2 wag		347.6	71	352.2	65	321.9	65	345.8	58
CH_2 rock		64.2	96	238.2	56	248.4	62	224.3	51

[a] Frequencies and infrared intensities are in cm^{-1} and km/mol. Observed frequencies are from argon matrix. Intensities are calculated values. [b] CCSD//6-311++G(2d,p)/SDD. [c] ADF//PW91. [d] B3LYP//6-311++G(3df,3pd)/SDD level of theory. [e] BPW91//6-311++G(2d,p)/SDD level of theory.

The sharp 1461.2 and 1425.4 cm^{-1} bands labeled **m** increase substantially together on UV irradiation and are in the range of agreement expected with the calculated U−H stretching frequencies for $CH_2{=}UH_2$. The upper symmetric stretching mode is weaker (38%) than the lower antisymmetric stretching mode, and our calculation also predicts it to be weaker (69%). We have no evidence for the substantially weaker infrared absorptions computed for modes in the 500−700 cm^{-1} region, but these modes were observed for the analogous halogen-substituted $CH_2{=}UHX$ complexes, which were produced in much higher yield.[63]

Reaction Energies and Mechanisms. Metal-atom methane-activation reactions proceed through bond insertion to form the methyl metal hydride.[16] Although this U + CH_4 reaction appears to be slightly endothermic at the CASPT2-SO level of theory, the insertion product decreases on annealing, but increases on UV irradiation (Figure 1). This indicates that reaction 1 is promoted by electronic excitation of U in the near-UV region.[64] The major triplet methylidene product is 1 kcal/mol higher in energy than the quintet insertion product at the CASPT2-SO level of theory, and the major growth of the triplet methylidene is also observed on UV irradiation. The overall reaction 1 is believed to proceed through the following mechanism: Electronically excited U* formed by ultraviolet irradiation activates CH_4 to form quintet $(CH_3{-}UH)^*$, which can be further excited to the quintet $(CH_2{-}UH_2)^*$ state following α-H transfer on the quintet potential-energy surface. The cold matrix then relaxes the energized quintet intermediate states to the quintet $CH_3{-}UH$ ground state and the triplet $CH_2{=}UH_2$ methylidene, and the methylidene dihydride complex appears to be the dominant product under these conditions. In the analogous Mo and methane system, ultraviolet irradiation produces more $CH_2{=}MoH_2$, a 12 kcal/mol higher energy species, than $CH_3{-}MoH$, and the analogous α-H transfer on the excited-quintet potential-energy surface mechanism has been proposed.[19a,b]

The **m** absorptions observed with CH_2D_2 are due to $CH_2{=}UD_2$ and $CD_2{=}UH_2$ as our calculations show that the U−H and U−D frequencies are not shifted from $CH_2{=}UH_2$ and $CD_2{=}UD_2$ values, respectively. The observation of the symmetric U−H and U−D stretching modes of $CD_2{=}UH_2$ and $CH_2{=}UD_2$ from the CH_2D_2 precursor (other bands masked by very strong precursor absorptions) can be explained by simple α-H transfer from the energized methyl uranium hydride first formed on the excited-quintet potential-energy surface.

$$\begin{array}{ccccc} U^* + CH_4 & \rightarrow & [CH_3{-}UH]^* & \rightarrow & [CH_2{-}UH_2]^* \\ & & \downarrow \text{ matrix relax} & & \downarrow \\ & & CH_3{-}UH & & CH_2{=}UH_2 \end{array} \quad (1)$$

$$U^* + CH_2D_2 \rightarrow [CHD_2{-}UH]^* \rightarrow [CHD{-}UHD]^* \rightarrow CHD{=}UHD \text{ and } CD_2{=}UH_2 \quad (2)$$

$$U^* + CH_2D_2 \rightarrow [CH_2D{-}UD]^* \rightarrow [CHD{-}UHD]^* \rightarrow CHD{=}UHD \text{ and } CH_2{=}UD_2 \quad (3)$$

If there were no agostic distortion, the U−H stretching mode of CHD=UHD would be the median of the two U−H stretching modes of $CH_2{=}UH_2$ (1443.3 cm^{-1} in this case). However, our calculations predict the U−H stretching modes for the distorted CHD=UHD isomers to be 8.2 and 33.5 cm^{-1} below the symmetric U−H stretching mode of $CH_2{=}UH_2$. We observe one of these weak absorptions at 1453.6 cm^{-1}, down 7.6 cm^{-1} from the observed symmetric mode, and the mode for the other isomer is presumably covered by the strong CH_2D_2 band at 1431 cm^{-1}. The weak band observed at 1453.6 cm^{-1} for CHD=UHD provides experimental evidence for agostic distortion of $CH_2{=}UH_2$, which is predicted by density functional, SOCI, and CASPT2 calculations and by comparison with $CH_2{=}ThH_2$ and $CH_2{=}MoH_2$.[16,17,19] On the basis of the calculated agostic C−H′ bond lengths and H′−C−M bond angles, the agostic distortion in $CH_2{=}UH_2$ is greater than in $CH_2{=}ThH_2$. Likewise, the agostic distortion computed for the $CH_2{=}UHX$ complexes is greater than that for the corresponding $CH_2{=}ThHX$ complexes.[63,65]

(63) Lyon, J. T.; Andrews, L. *Inorg. Chem.* **2006**, *45*, 1847 (U + CH_3X).
(64) Radziemski, L. J.; Steinhaus, D. W.; Engleman, R., Jr. *J Opt. Soc. Am.* **1971**, *61*, 1538.
(65) Lyon, J. T.; Andrews, L. *Inorg. Chem.* **2005**, *44*, 8610 (Th + CH_3X).

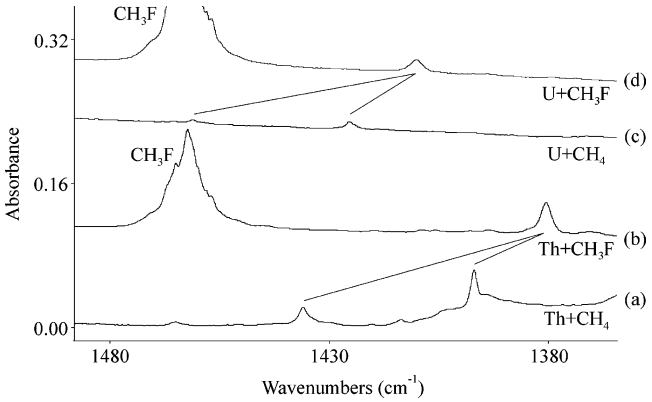

Figure 4. Infrared spectra in the actinide metal-hydride stretching region for laser-ablated U and Th reaction products with CH_4 and CH_3F in excess argon after ultraviolet irradiation and annealing at 32−35 K. (a) Th + 5% CH_4, (b) Th + 0.5% CH_3F, (c) U + 2.5% CH_4, and (d) Th + 0.5% CH_3F.

Spectra are compared in the actinide-hydrogen stretching region in Figure 4 for the U and Th methylidene dihydride and hydride fluoride systems.[17,63,65] Notice that the two An-H_2 stretching modes in $CH_2{=}UH_2$ and in $CH_2{=}ThH_2$ are slightly higher than the single An−H stretching mode in $CH_2{=}UHF$ and in $CH_2{=}ThHF$. Notice also that the U−H stretching frequencies are higher than corresponding Th−H stretching frequencies (25, 28, 30 cm^{-1}) by about the same amount that the antisymmetric fundamental of UH_4 (1484 cm^{-1}) is above this mode for ThH_4 (1445 cm^{-1}).[54,66] This frequency comparison between $CH_2{=}UH_2$ and $CH_2{=}UHF$, where U−H, U−F, and U−C stretching frequencies and CH_2 wagging modes were also observed,[63] substantiates our identification of $CH_2{=}UH_2$, the uranium methylidene dihydride.

The relative chemical reactivities are also revealed by the spectra in Figure 4, which were recorded under similar laser ablation conditions. Uranium appears to be less reactive than thorium with both CH_4 and CH_3F on the basis of product absorption intensities, but CH_3F is substantially more reactive than CH_4 (note the much-lower CH_3F concentrations employed). This we believe is due to the greater metal reactivity with the more electron-rich C−F subunit than with the C−H bond.

Structure and Bonding. It is of interest to compare the structures of $CH_2{=}ThH_2$ and $CH_2{=}UH_2$ and to understand the basis for the greater distortion for the uranium methylidene. Distortion of the CH_2 group in $CH_2{=}MH_2$ complexes appears to be a general characteristic of methylidene complexes of group 4, 5, and 6 metals, but in contrast, agostic distortion decreases in this transition metal series.[15−19] Slightly larger distortions have also been calculated at the DFT level for the $CH_2{=}UHX$ complexes than the analogous $CH_2{=}ThHX$ complexes.[63,65] This distortion is not likely to arise from electrostatic attraction of the metal center for the C−H-bonded electron pair because the ionization energies of Th and U are almost the same (6.1 eV),[67] and the Mulliken charges computed for the metal centers in these methylidene complexes are almost the same. We note, however, that the C=U bond is computed to be 0.06−0.08 Å shorter than the C=Th bond, and as a consequence, the U−agostic−H′ distance (2.178 Å) is considerably less than the Th−agostic−H′ distance (2.361 Å) (Figure 5). Recently, Andrews and Cho have shown from CCSD(T) calculations that stepwise relaxation of symmetry in $CH_2{=}ZrH_2$ leads to in-plane CH_2 and out-of-plane ZrH_2 distortion, whereas the C=Zr bond length decreases, and the electronic energy of the system decreases.[16] Similar behavior has been found here for $CH_2{=}ThH_2$, which has a distorted structure.[17] What then is responsible for the greater agostic distortion in U than in Th methylidene complexes? Hence, we examine structure and bonding analyses with both DFT and more rigorous CASSCF/CASPT2 methods for these actinide metals having different d and f orbital participations.

Figure 5 compares structures for $CH_2{=}ThH_2$ and $CH_2{=}UH_2$ calculated with two pure density functionals BPW91 and PW91 and CASPT2, and the agostic H′−C−M angle is consistently 4−6° smaller, and the C−H bond is 0.01 Å longer for the uranium than the thorium methylidene dihydride complex. Because the valence electron configurations of U($7s^25f^36d$) and Th($7s^26d^2$) are different, we expect different metal atomic orbital participations in the C−M sigma and pi bonds, and, accordingly, slightly different carbon orbital participations in the agostic C−H′ bond of interest here. We performed NBO analysis[68] of the bonding in both metal methylidene dihydrides at the BPW91 level of theory as provided by the Gaussian calculation, and the results are summarized in Table 3. The natural charges show that Th is slightly more positive, and thus carbon is slightly more negative, hence the higher carbon $2p^{4.15}$ character in $CH_2{=}ThH_2$ than the carbon $2p^{3.91}$ in $CH_2{=}UH_2$. The C−U σ bond contains about 4% less carbon 2s and 4% more carbon 2p character, and the C−U π bond has about 3% more carbon 2s and 3% less carbon 2p character as compared to the C−Th bond. The slightly longer agostic C−H bond for $CH_2{=}UH_2$ exhibits 0.9% more 2s and 0.7% less 2p character than for the agostic C−H bond in $CH_2{=}ThH_2$, but this must be considered in light of the overall carbon 2p character given above for the different actinide methylidenes. Thus, the longer agostic C−H bond is 2.88/3.91 = 0.736 of the available p character on C in $CH_2{=}UH_2$, whereas the shorter agostic C−H bond is 3.01/4.15 = 0.725 of the available p character on C in $CH_2{=}ThH_2$.

The CASSCF/CASPT2 calculations show that both actinide methylidenes are quite monoconfigurational, so DFT analysis should provide a good approximation. However, the more rigorous CASSCF/CASPT2 calculation serves as a calibration point for other methods. The pure DFT gives a more-polar molecule than CASSCF, which is traced back to the participation of 6d orbitals in the bonding and is much larger with CASPT2 than DFT. This gives less-polar bonds from metal to H and to C with the more rigorous method. The strong participation of 6d in Th and U bonds is a general

(66) Souter, P. F.; Kushto, G. P.; Andrews, L.; Neurock, M. *J. Phys. Chem. A* **1997**, *101*, 1287.
(67) *CRC Handbook of Chemistry and Physics: A Ready-Reference Book of Chemical and Physical Data*, 86th Edition; Lide, D. R., Ed.; Taylor & Francis: Boca Raton, FL, 2005 (IE of Th and U).
(68) Reed, A. E.; Curtiss, L. A.; Weinhold, F. *Chem. Rev.* **1988**, *88*, 899.

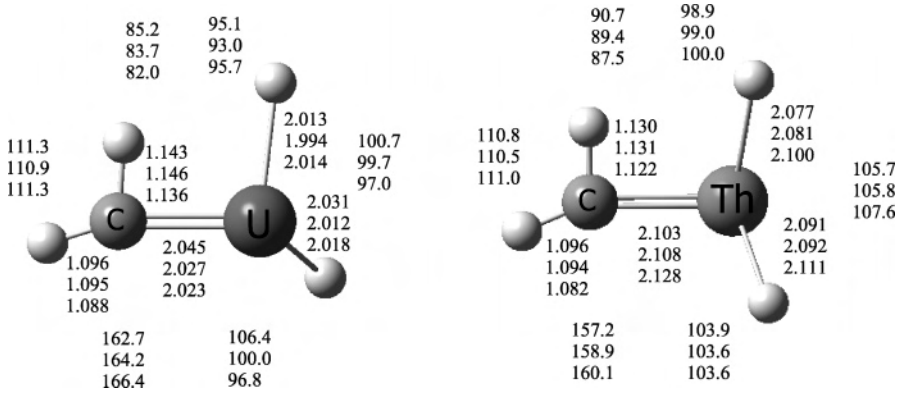

Figure 5. Structures calculated for $CH_2{=}UH_2$ and $CH_2{=}ThH_2$ using (a) the BPW91, (b) the PW91, and (c) the CASSCF/CASPT2 methods. Parameters (bond lengths in angstroms and angles in degrees) calculated by these three methods are given from top to middle to bottom, respectively.

Table 3. Computed Properties for $CH_2{=}UH_2$ and $CH_2{=}ThH_2$ from NBO Analysis and CASSCF/CASPT2 Calculations[a]

		$CH_2{=}UH_2$	$CH_2{=}ThH_2$
charge	M	2.14(2.295)	2.44
(spin density)		**0.70(2.144)**	
	C	−1.34(−0.213)	−1.61
		−0.70(−0.080)	
	H[b]	0.16(0.008)	0.18
		0.21(0.0039)	
	H[c]	0.20(0.003)	0.22
		0.19(−0.0005)	
	H[d]	-0.57(−0.044)	−0.61
		−0.020(−0.033)	
	H[e]	−0.59(−0.050)	−0.62
		−0.20(−0.034)	
natural	M	$7s^{0.42}\ 5f^{2.73}$	$7s^{0.44}\ 5f^{0.28}$
electron config.		$6d^{0.75}\ 7p^{0.02}$	$6d^{0.87}\ 7p^{0.03}$
		$7s^{0.44}\ 5f^{2.31}$	**$7s^{0.64}\ 5f^{0.43}$**
		$6d^{2.22}\ 7p^{0.09}$	**$6d^{2.36}\ 7p^{0.03}$**
	C	$2s^{1.41}\ 2p^{3.91}$	$2s^{1.42}\ 2p^{4.15}$
		$3p^{0.01}\ 3d^{0.01}$	$3p^{0.01}\ 3d^{0.03}$
	H[b]	$1s^{0.83}$	$1s^{0.82}$
	H[c]	$1s^{0.79}$	$1s^{0.78}$
	H[d]	$1s^{1.57}$	$1s^{1.61}$
	H[e]	$1s^{1.59}$	$1s^{1.61}$
bond character	M−C σ	U s(3.6%) p(1.9%)	Th s(4.5%) p(3.6%)
from NBO		d(40.2%) f(54.1%)	d(68.8%) f(23.1%)
		C s(20.7%) p(79.2%)	C s(24.4%) p(75.3%)
	M−C π	U s(7.1%) p(1.8%)	Th s(9.5%) p(2.8%)
		d(38.6%) f(52.5%)	d(62.9%) f(24.8%)
		C s(12.7%) p(87.2%)	C s(9.6%) p(89.9%)
	C−H[b]	C s(25.7%) p(73.8%)	C s(24.8%) p(74.5%)
	C−H[c]	C s(40.7%) p(59.1%)	C s(41.0%) p(58.8%)

[a] BPW91//6-311++G(2d,p)/SDD level of theory with CASSCF/CASPT2 in bold type. [b] Agostic hydrogen attached to carbon. [c] Second hydrogen attached to carbon. [d] Hydrogen attached to metal center cis to agostic hydrogen. [e] Hydrogen attached to metal center trans to agostic hydrogen.

feature, and it fits well with other results such as the actinide dimers.[69]

It is significant that CASSCF/CASPT2 shows a direct interaction between the U(5f) sigma open-shell orbital and the agostic hydrogen. This interaction has shifted the spin density on the hydrogen from the normal negative polarization density to be slightly positive. This open-shell interaction is plotted at different electron densities in Figure 3B, and at the most sensitive level, we see the delocalization of electron density onto the agostic hydrogen. Hence, we conclude that more favorable interaction with the lower-energy open-shell U(5f) orbital is responsible for the stronger agostic interaction in the U methylidene than found for the higher-energy vacant Th (6d) orbital in the Th methylidene dihydride molecules, as has been discussed in more detail in a theoretical comparison of $CH_2{=}MH_2$ complexes.[19c]

Finally, our DFT calculations locate a stable singlet $CH{\equiv}UH_3$ molecule with C_{3v} symmetry and higher energy (47, 30, 34, and 54 kcal/mol at the B3LYP, PW91, CASPT2, and CASPT2-SO levels) than triplet $CH_2{=}UH_2$. This $CH{\equiv}UH_3$ molecule contains a nice, although slightly long, triple bond with one sigma and two pi orbitals. The very strong U−H stretching modes predicted near 1500 cm^{-1} for $CH{\equiv}UH_3$ were not observed here. Apparently, its much higher energy makes $CH{\equiv}UH_3$ an unlikely product in contrast to $CH{\equiv}MoH_3$ and $CH{\equiv}WH_3$, which have stronger metal−hydride bonds and energies comparable to the other products in the group 6 metal systems.[19a,b] The computed structures for singlet $CH{\equiv}UH_3$ are compared in Figure 2 at the B3LYP, PW91, and CASSCF/CASPT2 levels of theory. Notice the very good agreement among the DFT and multiconfiguration methods for this singlet molecule. Although B3LYP/Gaussian predicts the U−H stretching frequencies more accurately, PW91/ADF provides structures in better agreement with the more-rigorous CASSCF/CASPT2 methods.

Conclusions

Ultraviolet excitation of uranium atoms promotes reaction with methane to form the methyl uranium hydride CH_3−UH and its α-H transfer product uranium methylidene dihydride, $CH_2{=}UH_2$. These methane activation products are identified from the matrix infrared spectrum in the U−H stretching region through isotopic substitution ($^{13}CH_4$, CD_4, CH_2D_2) and density functional theory frequency calculations. Higher-level CASSCF/CASPT2 calculations demonstrate that the triplet $CH_2{=}UH_2$ ground-state molecule has a distorted structure of the type associated with agostic bonding, which we associate with stabilization of the C=U double bond owing to the involvement of U(5f) valence orbitals. DFT with the B3LYP functional in the Gaussian system and the

(69) Roos, B. O.; Malmqvist, P.-Å.; Gagliardi, L. *J. Am. Chem. Soc.* **2006**, *105*, 17000.

PW91 functional using the ADF code provide good predictions of the vibrational spectrum of $CH_2{=}UH_2$.

Agostic distortion in triplet state $CH_2{=}UH_2$ is enhanced by the shorter C═U bond and the lower energy, compact open shell U(5f) orbital interaction with the agostic hydrogen. The CASSCF/CASPT2 calculation shows that the U(5f) σ orbital interacts with the agostic hydrogen, which is revealed by electron density plots at more sensitive levels and significant agostic structural distortion. The C═Th bond is longer and the Th (6d) orbital is higher in energy, which sustains a weaker interaction and supports less agostic distortion.

Acknowledgment. We gratefully acknowledge financial support for this research from NSF grant no. CHE 03-52487 and the Donors of the American Chemical Society Petroleum Research Fund to L. A and from the Swedish Science Research Council (VR) to B.O.R. and P.-Å.M. We thank the William R. Wiley Environmental Molecular Sciences Laboratory (EMSL) and the Ohio State Supercomputer Center for computer time and H.-G. Cho for performing the CCSD frequency calculation on $CH_2{=}ThH_2$.

IC062407W